ACS Medicinal Chemistry Letters

Letter

pubs.acs.org/acsmedchemlett

Selective Acetamidine-Based Nitric Oxide Synthase Inhibitors: Synthesis, Docking, and Biological Studies

Cristina Maccallini,*[,†] Monica Montagnani,[‡] Roberto Paciotti,[†] Alessandra Ammazzalorso,[†] Barbara De Filippis,[†] Mauro Di Matteo,[†] Sara Di Silvestre,[§] Marialuigia Fantacuzzi,[†] Letizia Giampietro,[†] Maria A. Potenza,[‡] Nazzareno Re,[†] Assunta Pandolfi,[§] and Rosa Amoroso*[,†]

[†]Department of Pharmacy, University of Chieti "G. d'Annunzio", 66100 Chieti, Italy

[‡]Department of Biomedical Sciences and Human Oncology, Medical School, University of Bari "Aldo Moro", 70121 Bari, Italy

[§]Department of Medical, Oral and Biotecnological Sciences, University "G. d'Annunzio" Aging Research Center, "G. d'Annunzio" University Foundation, 66100 Chieti-Pescara, Italy

Supporting Information

ABSTRACT: *N*-[(3-Aminomethyl)benzyl]acetamidine derivatives were synthesized and *in vitro* evaluated as inhibitors of the inducible isoform of nitric oxide synthase (iNOS). Because of the high potency of action and the excellent selectivity over the endothelial nitric oxide synthase (eNOS), compound **10** was *ex vivo* evaluated on isolated and perfused resistance arteries. The results confirm that compound **10** selectively inhibits the iNOS, without affecting the endothelial isoform. The outcome of the docking studies showed that the hydrophobic interaction is the driving force of the binding process, especially for iNOS, where the binding pocket is characterized by a significant lipophilic region.

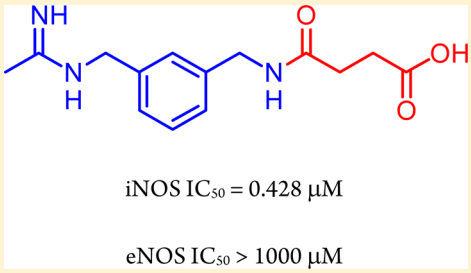

iNOS IC_{50} = 0.428 μM

eNOS IC_{50} > 1000 μM

KEYWORDS: *Acetamidine, inhibitor, molecular docking, nitric oxide synthases, synthesis, selective*

Nitric oxide (NO) is a highly diffusible pleiotropic molecule, involved in the regulation of many biological processes. It is biosynthesized from L-arginine (L-Arg) by nitric oxide synthase (NOS), in a two step reaction involving oxygen, reduced nicotinamide adenine dinucleotide phosphate (NADPH), and many other cofactors. An essential prerequisite for NOS activity is the enzyme dimerization, which requires the cofactor tetrahydrobiopterin (BH_4).[1] Under physiological conditions, the so-called "NO tone" (i.e., the production of basal NO levels) is mediated by two constitutive NOS isoforms: the endothelial one (eNOS), mainly expressed in vascular endothelial cells and responsible for the vasculature homeostasis,[2] and the neuronal one (nNOS), which is involved in neurotransmission.[3] A third NOS isoform, inducible NOS (iNOS), plays an important role in the defense against pathogens and is expressed in several cells and tissues, including endothelial and vascular smooth muscle cells,[4] in response to pro-inflammatory stimuli such as bacterial endotoxins (LPS), and/or different cytokines and interleukins.[5] In contrast to the regulated production of NO by eNOS and nNOS, iNOS may generate large amounts of NO over long periods of time, if substrate and cofactors are not limited.[4] In the vascular system, the excessive amount of NO produced by iNOS is associated with decreased function of eNOS and subsequent impairment of both vasoconstriction and endothelium-dependent vasorelaxation.[6,7] Furthermore, the iNOS-dependent detrimental overproduction of NO and related species such as peroxynitrites are implicated also in pathophysiological conditions such as asthma,[8] hypertension,[9] inflammatory bowel disease,[10] and cancer.[11,12] Selective inhibition of iNOS could therefore represent a feasible therapeutic strategy to treat the aforementioned and other conditions, and intense efforts to identify selective iNOS inhibitors have been carried out.[13] According to their different mechanism of action, these compounds may be divided into two major groups: molecules targeting the L-Arg binding site and acting as competitive inhibitors of the natural substrate, and inhibitors of the enzyme dimerization.[14] The first class of compounds is characterized by the presence of a guanidine-like moiety, able to mimic the L-Arg guanidine−protein interactions in the binding site. Owing to their structural similarities with L-Arg, earlier substrate-competitive inhibitors block the three isoforms indiscriminately, with unacceptably severe side effects. Later, several selective non amino acid iNOS inhibitors were disclosed, many of which are amidines showing remarkable potency and selectivity of action.[15] In this context, we previously identified new acetamidines able to inhibit iNOS with a very high selectivity profile over eNOS or nNOS.[16−19] In particular, within a series of compounds structurally related to the selective iNOS inhibitor *N*-[(3-aminomethyl)benzyl]-acetamidine (1400W),[20] we found that compounds **1** and **2** showed encouraging *in vitro* activity against iNOS (IC_{50} = 0.1 ±

Received: November 11, 2014
Accepted: April 28, 2015
Published: April 28, 2015

DOI: 10.1021/acsmedchemlett.5b00149
ACS Med. Chem. Lett. 2015, 6, 635−640

0.01 and 0.5 ± 0.04, respectively) and high selectivity over eNOS (Figure 1). A docking study revealed that the benzyl tail

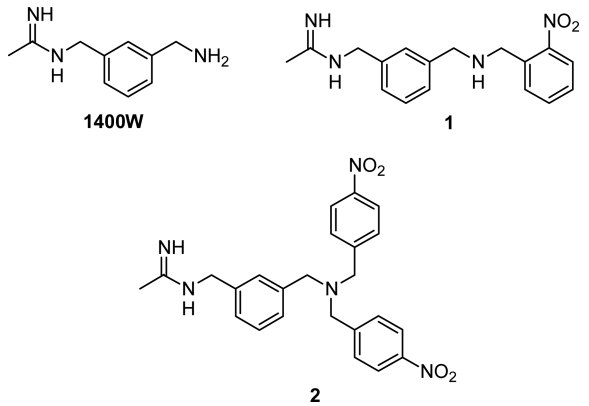

Figure 1. Structures of 1400W and its benzyl derivatives **1** and **2**.

of **1** and **2** extends in the substrate access channel, where the major differences between NOS isoforms are localized. Indeed, this specific interaction is responsible for the observed activity and selectivity,[18] confirming that the most important determinants for the potency and selectivity of the NOS inhibitors are hydrophobic and charge−charge interactions.[21]

On this basis, we designed compounds **9**−**14** (Figure 2), showing the *N*-[(3-aminomethyl)benzyl]acetamidine scaffold

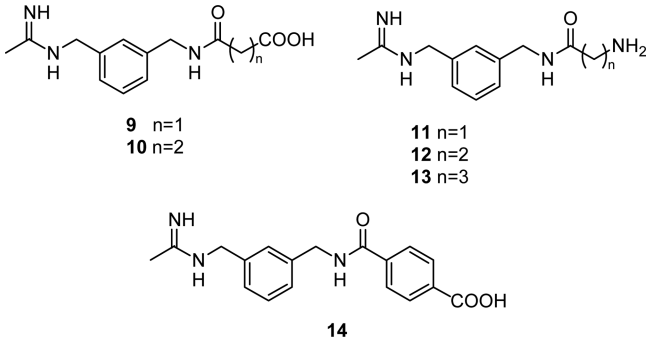

Figure 2. Target molecule structures.

linked to an amidoalkyl or amidoaryl moiety, ending with a carboxylic or amino group. What we expected was that the hydrocarbon chain of these ligands could provide hydrophobic contacts, while the ionizable group, exploiting differences between the isoform non conserved residues, could play a role in the selectivity toward the eNOS. Here we report the synthesis of compounds **9**−**14**, together with their *in vitro* activity and selectivity. Biological activity and physiological relevance of selective iNOS inhibition were further evaluated *ex vivo* on isolated and perfused resistance arteries. Finally, insights from a docking study are also discussed.

Synthesis of **9**−**13** was performed according to Scheme 1. Monoterbutyl esters of malonic and succinic acids and the BOC protected amino acids Gly, *β*-Ala, and GABA were coupled with *N*-[(3-aminomethyl)benzyl]acetamidine,[21] giving intermediates **3**−**7**. Acidolysis of **3**−**7** protecting groups generated final products **9**−**13**. In order to synthesize **14**, methyl terephthaloyl chloride was coupled with 1400W affording intermediate **8**, which was then hydrolyzed to give the desiderate compound (Scheme 2).

Scheme 1. Synthesis of 9−13[a]

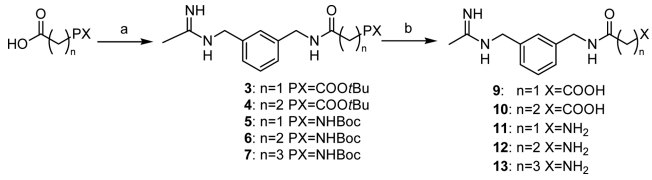

[a]Reagents and conditions: (a) 1400W, *i*BuOCOCl, NMM, DMF_{dry}, N_2, 0 °C to r.t., 24 h; (b) 4 N HCl, dioxane, r.t., 24 h.

Scheme 2. Synthesis of 14[a]

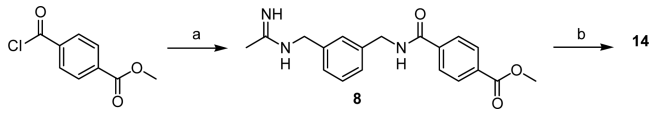

[a]Reagents and conditions: (a) 1400W, TEA, DMAP, DMF_{dry}, N_2, 0 °C, 6 h; (b) 4 N HCl, dioxane, r.t., 24 h.

The synthesized compounds were evaluated for their *in vitro* NOS inhibitory activities by measuring the conversion of [^{3}H]L-arginine to [^{3}H]L-citrulline ([^{3}H]L-Cit), using a radiometric method (Table 1). Compound **9**, which contains a

Table 1. Inhibition of iNOS and eNOS by 9-14: IC_{50} and Selectivity

	IC_{50}[a] (μM)		
compd	iNOS	eNOS	eNOS/iNOS selectivity
9	>10	n.d.	
10	0.428 ± 0.032	>1000	>2300
11	>10	n.d.	
12	>10	n.d.	
13	>10	n.d.	
14	0.165 ± 0.008	90.8 ± 7.2	550
1	0.1 ± 0.01[18]	30 ± 2.5[18]	300
2	0.5 ± 0.04[18]	100 ± 8.1[18]	200
1400W	0.1 ± 0.095	350 ± 2.4	3500

[a]Values given are mean ± SD of experiments performed in triplicate at seven different concentrations.

malonyl residue, was quite inactive against iNOS (IC_{50} >10 μM), but interestingly, the homologous compound **10**, containing a succinyl residue, proved to be a potent iNOS inhibitor (IC_{50} = 0.428 μM) with an excellent degree of selectivity with respect to eNOS (IC_{50} > 1000 μM; eNOS/iNOS selectivity ratio >2300-fold). The introduction of the therephthalic residue in compound **14** gave a more potent iNOS inhibitor (IC_{50} = 0.165 μM), albeit less selective (eNOS IC_{50} = 90.8 μM; eNOS/iNOS selectivity ratio 550-fold). Comparing these results to potency and selectivity of the parent compounds **1** and **2**, it appears that the main advantage of the new molecules is their higher selectivity toward iNOS. Anyway, in comparison with 1400W, new molecules are less selective, albeit it could be hypothesized that **10** is endowed with a similar selectivity compared to the lead compound (>2300-fold vs 3500-fold). Molecules **11**−**13**, containing an ending amino group instead of the carboxylic one, were quite inactive against iNOS. These results, supported by docking study, suggest that, limited to the molecular scaffold used, the carboxylic residue plays a positive role in anchoring the inhibitors into the iNOS binding site.

DOI: 10.1021/acsmedchemlett.5b00149
ACS Med. Chem. Lett. 2015, 6, 635−640

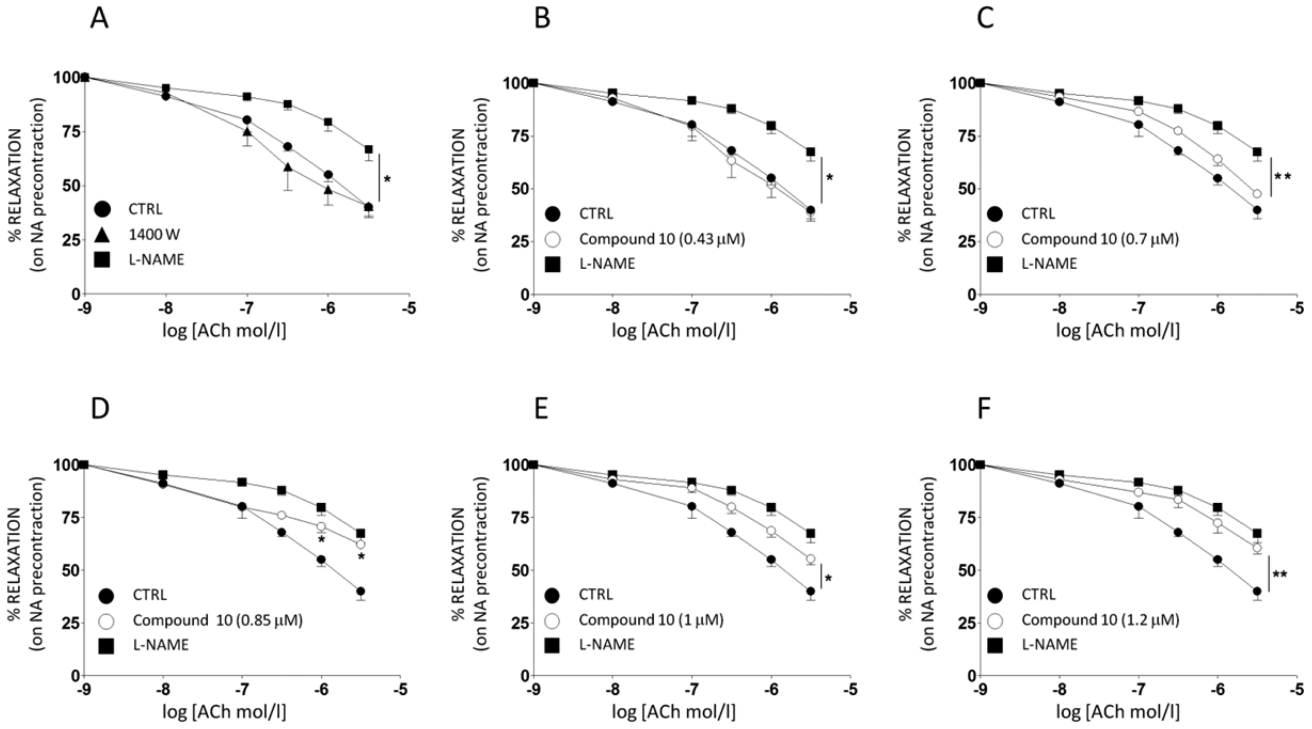

Figure 3. Effects of compound **10** on ACh-mediated NO-dependent vasodilation. Mesenteric vascular arteries (MVA) isolated from SD rats were contracted to ∼80% of maximal vasoconstriction with 10 μM NA. (A) Dose−response curves for ACh-induced vasorelaxation (0.01−3 μM/30 s) were obtained in MVA under control conditions and after pretreatment with 1400W (1 μM) and subsequent treatment with L-NAME (100 μM). (B−F) Dose−response curves for ACh-mediated vasorelaxation were obtained in MVA under control conditions, and after pretreatment with increasing concentrations of compound **10** and subsequent treatment with L-NAME. Results are mean ± SEM of duplicates from four independent experiments for each condition. Asterisks refer to significant differences found between indicated curves assessed by two way ANOVA for repeated measures. *p < 0.05; **p < 0.01 vs L-NAME (panels A−C) or CTRL (panels D−F) curves, respectively.

Because of the promising *in vitro* results, chemical and enzymatic stability of **10** were assessed. Phosphate buffer (pH = 7.4), HCl solution (pH = 2.0), NaOH solution (pH = 9.0), and human plasma were adopted as media. Immediately after dissolution and at appropriate time intervals, 5 μL of each solution was withdrawn and injected into an HPLC apparatus (Waters, Milford, USA), equipped with a X-Terra C_8 column (Waters), eluted using a mixture of H_2O/CH_3CN/TFA (25:75 + 0.1%) and revealed by means of a photodiode array. Solutions were kept at 37 °C and monitored for 24 h. Compound **10** proved to be stable in each of the considered medium, as no loss of product was observed.

Ex vivo assays were then performed to deepen **10** selectivity profile. In healthy vessels, where iNOS is not expressed, the selectivity of a prospective iNOS inhibitor may be inferred from its inability to reduce NO-mediated (eNOS-dependent) vasodilation. Since acetylcholine (ACh) administration leads to eNOS activation and subsequent NO-mediated vasodilation in rat isolated mesenteric arteries,[22] inhibition of ACh-mediated vasorelaxation was evaluated in the absence and in the presence of **10**. The obtained dose−response curves were compared with those produced under 1400W and N^{ω}-nitro-L-arginine methyl ester (L-NAME), a selective and unselective NOS inhibitor, respectively (Figure 3A). As expected, treatment with 1400W (1 μM/30 min preincubation) did not affect the ACh-induced vasodilation, whereas L-NAME (100 μM/30 min preincubation) was able to significantly inhibit the vasodilator effect produced by ACh at all doses tested (Figure 3A; *p < 0.01 vs CTRL). Compound **10** was preincubated for 30 min at concentrations starting from 0.43 μM (IC_{50} value) and up to 1.2 μM, and its ability to modify ACh-mediated vasodilation was compared to that elicited by subsequent administration of L-NAME. At 0.43 μM (Figure 3B) and up to 0.7 μM concentration (Figure 3C), **10** did not exert any significant effect on vasodilation in response to ACh. Indeed, under these conditions, ACh-mediated vasodilation curves in CTRL and compound **10** groups were comparable. Conversely, L-NAME almost completely abrogated ACh-mediated vasodilation (Figure 3B, p < 0.05; C, p < 0.01 vs respective compound **10** curves). When the vessels were coinfused with **10** at concentrations of 0.85 μM (Figure 3D), a substantial decrease was observed for vasodilation elicited by the higher doses of ACh (p < 0.05 vs respective CTRL curve). Starting from concentrations of 1 μM (Figure 3E) and up to 1.2 μM (Figure 3F), **10** was able to lessen ACh-dependent relaxation (*p < 0.05; **p < 0.01 vs respective CTRL curve), with no additional difference with respect to the inhibitory effect produced by L-NAME (Figure 3E-F). Thus, in line with results from experiments *in vitro*, concentrations of **10** up to 0.7 μM did not interfere with physiological activity of eNOS *ex vivo*. Compound **10** eNOS/iNOS selectivity was then tested in vessels from rats treated with bacterial lipopolysaccharide (*E. coli* LPS, 30 mg kg^{-1}, i.p.). The endotoxin-induced septic shock is characterized by hyporeactivity to noradrenaline (NA)-mediated vasoconstriction that depends on dysregulated synthesis and release of several vascular mediators, including IL-1β, TNFα, IL-10, and cyclooxygenase-2-mediated prostacyclin. Nevertheless, the abnormal production of NO generated by iNOS remains a crucial element in the cardiovascular dysfunction of LPS-treated rats.[23] Overexpression of iNOS was

DOI: 10.1021/acsmedchemlett.5b00149
ACS Med. Chem. Lett. 2015, 6, 635−640

observed in the homogenate of aortas isolated from LPS-treated rats (Figure 4A). Dose−response curves to NA (10 nM−10 μM), obtained in mesenteric vessels from LPS-treated rats were compared to NA curves obtained under subsequent administration of **10** (0.43 μM/30 min), L-NAME (100 μM/30 min), and 1400W (1 μM/30 min) (Figure 4). When compared to CTRL curve, the maximal vasoconstrictor effect (peak effect) induced by individual doses of NA was slightly but significantly increased after preincubation with **10** (Figure 4B, $*p < 0.05$). This ameliorated NA-induced contraction was comparable to that obtained under incubation with the selective iNOS inhibitor 1400W (Figure 4B). With respect to both **10** and 1400W, L-NAME treatment induced a much higher increase in NA-mediated vasoconstriction (Figure 4B, $p < 0.001$ vs CTRL; $^{\circ}$ $p < 0.01$ vs compound 10). Similarly, when compared to basal conditions, the total extent of vasoconstriction induced by NA (AUC) was substantially increased by **10** and 1400W (Figure 4C: * $p < 0.01$ vs CTRL), and further enhanced by treatment with L-NAME (Figure 4C: $*p < 0.001$ vs. CTRL; $^{\circ}$ $p < 0.01$ vs compound **10**). Thus, biological properties from *ex vivo* conditions strongly support the idea that **10** has a selective inhibitory activity (resembling that of 1400W) toward iNOS isoforms.

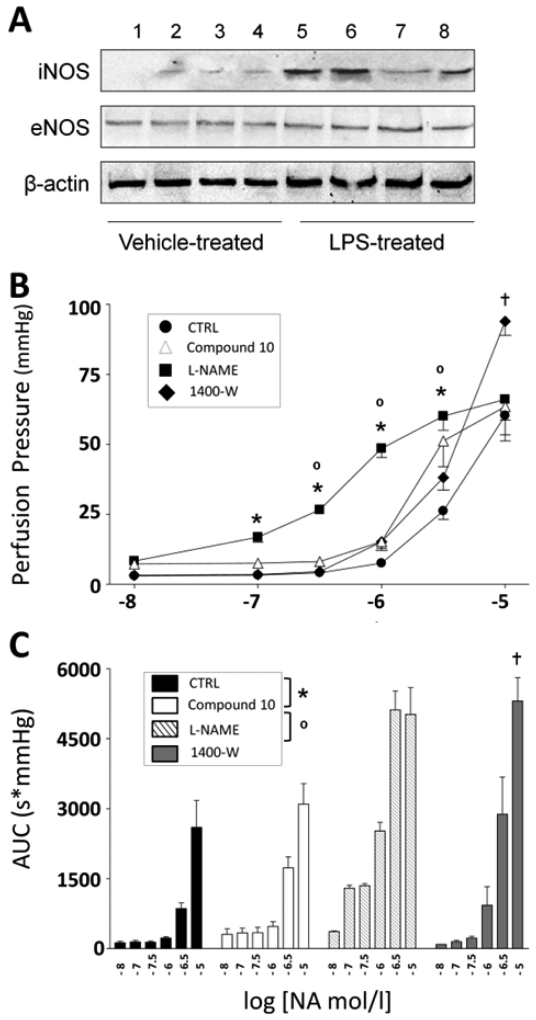

Figure 4. Effects of compound **10** on NA-induced vasoconstriction. (A) Aortas were isolated from SD rats injected with vehicle or LPS. Samples were homogenized and subjected to immunoblotting with iNOS, eNOS or β-actin antibodies. Representative blot shows overexpression of iNOS from vessels of LPS-treated, but not of vehicle-treated animals. (B) Dose−response curves for NA-induced vasoconstriction (10 nM−10 μM) were obtained in MVA under basal conditions (CTRL), after pretreatment with compound **10**, and after subsequent treatment with L-NAME and 1400W. Maximal vasoconstriction to individual NA doses (peak effect) was measured as perfusion pressure value and expressed in mmHg. (C) Duration of vasoconstriction obtained with individual NA doses (10 nM−10 μM) was calculated as area under the curve (AUC) and expressed as perfusion pressure (mmHg) × time (sec). Values were compared among curves obtained under CTRL conditions, pretreatment with compound **10**, and subsequent pretreatment with L-NAME and 1400W. Results are mean ± SEM of duplicates from four independent experiments repeated for each condition. Symbols refer to significant differences between NA doses under treatment with compound **10** vs CTRL ($*p < 0.05$), vs L-NAME ($^{\circ}p < 0.05$), and 1400W ($^{\dagger}p < 0.05$), respectively.

To shed light on the structural basis for the evaluated potencies and selectivities, we preliminarily considered **9**−**14** lipophilicity by calculating logP (*n*-ottanol/water) with MoKa software.[24,25] As expected, ligand lipophilicity increased with the growth of the hydrocarbon spacer between the amide and the terminal carboxylic/amino groups. Calculated logP values are −0.75 for **9**, −1.08 for **11**, −0.28 for **10**, −0.76 for **12**, −0.26 for **13**, and 1.89 for **14**, and Table S2 in Supporting Information summarizes such a relationship between the growth of spacer unit in acyl moiety and the ligand lipophilicity.

Subsequently, a molecular docking study of **9**, **10**, and **14**, into eNOS and iNOS binding sites, was performed. The structure of the two isoforms eNOS and iNOS was prepared by means of Protein Preparation Wizard,[26] starting from 1FOI and 1QW5 pdb files, respectively. Docking calculations were performed employing the XP approach implemented in Glide,[26] and results are summarized in Table 2 together with the most significant contributions to the XP G score function.[25] The best ranking poses of **14** are shown in Figure 5 (other docking poses in SI).

Similarly to 1400W (see for instance 1QW5 pdb file), all the ligands interact with the Glu371(2) and Trp366(1) residues of the iNOS binding site through their acetamidine moiety, forming two and one H-bonds, respectively. Compounds **9** and **10** show additional interactions of the acyl group, forming two more hydrogen bonds, one with residue Asn348 and one with the propionate group of heme. On the other hand, compound **14** shows no additional hydrogen bonds, but the phenyl spacer shows good contacts in the lipophilic region. It is worth noting that, although **9** and **10** have a more favorable H-bond contribution, **14** has a higher Lipophilic EvdW contribution and, at variance with **9** and **10**, shows no conformational penalty in the binding pose. This result can be visually appreciated superimposing the ligand poses with the SiteMap[25] fields (see Figures in SI): **14** better interacts with the lipophilic region, and moreover, the terephthalyl moiety is planar, so that the π electrons are delocalized on all the π-system (amide−benzene−carboxylate), thus justifying the lack of a conformational penalty. The 1400W core of **10** docking pose also better interacts with the lipophilic region, but although the aliphatic chain of succinyl moiety is located near the lipophilic region, the alpha C atom has a negative partial charge, resulting in a bad contact. Moreover, the CH_2−CH_2 unit shows a gauche conformation consistent with RotPenalty of 0.983. Finally, **9** has the less favorable XP Lipophilic EvdW and the highest XP RotPenalty contributions; in the docking pose the benzene moiety does not properly fit the lipophilic area, and the partial

DOI: 10.1021/acsmedchemlett.5b00149
ACS Med. Chem. Lett. 2015, 6, 635−640

Table 2. Most Important Terms of XP Gscore Function, Experimental IC_{50} and Calculated logP(*n*-Ottanol/Water) for 9, 10, and 14

	iNOS			eNOS		
properties	14	10	9	14	10	9
IC_{50} (μM)	0.1651	0.4279	>10	90.82	>10	>10
$-\log(IC_{50})$	0.7822	0.3687	n.a.	−1.9582	n.a.	n.a.
XP Gscore	−10.073	−9.540	−8.735	−9.998	−9.335	−8.637
XP Hbond	−1.976 (3)[a]	−2.439 (5)	−2.406 (5)	−2.815(6)	−3.026(7)	−2.639 (6)
XP Lipohilic EvdW	−2.733	−2.285	−1.605	−1.966	−1.633	−1.610
XP RotPenal	0.000	0.983	1.076	0.372	1.124	1.076
Emodel	−84.296	−81.657	−76.840	−80.296	−73.634	−66.537
glide EVdW	−30.901	−28.311	−26.356	−25.808	−24.152	−24.482
log P (*n*-ottanol/H_2O)	1.89	−0.28	−0.75	1.89	−0.28	−0.75

[a]Values in parentheses are the total number of ligand−receptor H-bonds.

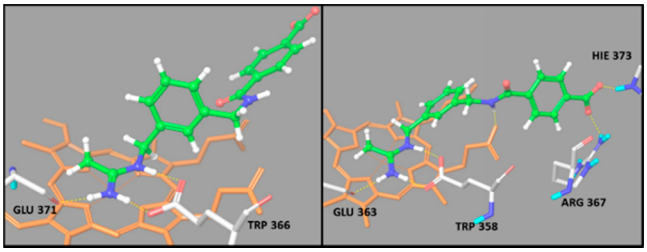

Figure 5. Best ranking pose of **14** in (left) iNOS and (right) eNOS binding sites. The H-bonds between ligand and receptor are represented by yellow dotted lines; in gray the side chains involved in H bonds with ligand, and in orange the cofactor heme.

negative charged C alpha is immersed into hydrophobic region leading to an unfavorable interaction. Moreover, the malonyl moiety is characterized by an eclipsed conformation, as reflected by the high rotational penalty value.

All three ligands also interact with the eNOS binding site through the Glu363(2) and Trp358(1) residues, forming three H-bonds. Ligand **14** forms three more H-bonds through the Hie373(1) and Arg367(1) residues and the propionic group of heme cofactor; **10** forms four more H-bonds with Arg374(2) and Hie373(1) residues and the propionic group of heme(1); **9** forms three more interactions with Ser248(1) and Gln249(2). However, the hydrocarbon spacer of the acyl moiety points in the H-bond acceptor region of binding site rather than in the lipophilic region and cannot establish the hydrophobic stabilizing interactions observed in iNOS. The order of the calculated XPscore and Emodel function[25] for the docking of **14**, **10**, and **9** to eNOS are in agreement with experimental data. Moreover, the values of XPscore and Emodel function for the docking to eNOS, in particular the XP Lipophilic EvdW term, are lower than the corresponding values for the docking to iNOS, in line with the observed selectivity. These results are consistent with SiteMap calculations (see Table S3 in SI): the lipophilic area of eNOS binding pocket is smaller (142.1 $Å^2$) and the hydrophobic interaction has the same importance of the hydrophilic one (balance = 0.91), even if the latter is slightly more relevant (Phili = 1.16 against Phobic = 1.06).

In this situation, only a part of the ligand can fit the hydrophobic region, justifying the smallest contribution of the XP Lipophilic EvdW to the final XP Gscore function. The importance of the H-bonds in eNOS binding site is highlighted by the values of XP H-bond terms, which are higher for eNOS rather than iNOS. The XP RotPenalty terms calculated for eNOS binding site are higher than the values obtained for iNOS for all ligands; in particular the π-system (amide−benzene−carboxylate) of **14** is not planar, breaking the π-electron delocalization, while the acyl moieties of **10** and **9** have an almost eclipsed conformation. Taking into account the Emodel function also allows to reproduce the relative selectivity of the three ligands. Indeed, the values of Emodel for the binding to eNOS is significantly lower than that for the binding to iNOS, and the largest difference for **10** is consistent with the experimental data, showing for this ligand the highest eNOS/iNOS selectivity ratio.

A docking investigation was also performed for **11**−**13** into iNOS and eNOS binding sites (results in Table S4 and Figure S4 in Supporting Information) to try to understand why the biological activity dramatically changes by replacing the negative carboxylate group with positive ammonium group. The analysis of docking poses reveals that the ammonium group is placed in the donor H bond region, located exactly on the opposite side of the lipophilic surface. Consequently, for **11**−**13**, the alkyl chain is forced in the hydrophilic region, far from hydrophobic surface, thus reducing the binding efficiency. Conversely, for **9**, **10**, and **14**, the negatively charged carboxylic group is placed in the acceptor H-bond region, which is located adjacent to the lipophilic region, thus allowing the hydrocarbon chain to point toward it and stabilize the interaction.

In summary, we have disclosed new potent and selective iNOS inhibitors. Compounds **10** and **14** showed submicromolar activities (0.428 and 0.165 μM, respectively) and excellent selectivity over eNOS (>2300- and 550-fold, respectively). Altogether, findings from *in silico*, *in vitro*, and *ex vivo* procedures reveal promising properties for these molecules and support a potential role for future therapeutic applications.

■ ASSOCIATED CONTENT

Supporting Information

Synthetic procedures, full characterization of the synthesized compounds, HPLC separation conditions, biological assay protocols, computational details, and docking poses. The Supporting Information is available free of charge on the ACS Publications website at DOI: 10.1021/acsmedchemlett.5b00149.

■ AUTHOR INFORMATION

Corresponding Authors

*E-mail: cmaccallini@unich.it. Fax: +39 0871 3554681.
*E-mail: ramoroso@unich.it. Fax: +39 0871 3554681.

DOI: 10.1021/acsmedchemlett.5b00149
ACS Med. Chem. Lett. 2015, 6, 635−640

Funding

This study was supported by University "G. d'Annunzio" of Chieti local grants.

Notes

The authors declare no competing financial interest.

■ ABBREVIATIONS

NO, nitric oxide; L-Arg, L-arginine; NOS, nitric oxide synthases; NADPH, reduced nicotinamide adenine dinucleotide phosphate; BH_4, tetrahydrobiopterin; eNOS, endotelial nitric oxide synthase; nNOS, neuronal nitric oxide synthase; iNOS, inducible nitric oxide synthase; LPS, bacterial lipopolysaccaride; 1400W, *N*-[(3-aminomethyl)benzyl]acetamidine; BOC, *tert*-butyloxycarbonyl; *β*-Ala, *β*-alanine; Gly, glycine; GABA, *γ*-aminobutirryc acid; *i*BuOCOCl, *iso*-butylchloroformate; NMM, *N*-methyl-morpholine; DMF, *N*,*N*-dimethylformamide; TEA, triethylamine; DMAP, dimethylaminopyridine; IC_{50}, half maximal inhibitory concentration; ACh, acetylcholine; L-NAME, N^{ω}-nitro-L-arginine methyl ester; CTRL, control; NA, noradrenaline; AUC, area under the curve

■ REFERENCES

(1) Santolini, J. The molecular mechanism of mammalian NO-synthases: A story of electrons and protons. *J. Inorg. Biochem.* **2011**, *105*, 127−141.
(2) Förstermann, U.; Li, H. Therapeutic effect of enhancing endothelial nitric oxide synthase (eNOS) expression and preventing eNOS uncoupling. *Br. J. Pharmacol.* **2011**, *164*, 213−223.
(3) Zhou, L.; Zhu, D. Y. Neuronal nitric oxide synthase: structure, subcellular localization, regulation, and clinical implications. *Nitric Oxide* **2009**, *20*, 223−230.
(4) Pautz, A.; Art, J.; Hahn, S.; Nowag, S.; Voss, C.; Kleinert, H. Regulation of the expression of inducible nitric oxide synthase. *Nitric Oxide* **2010**, *23*, 75−93.
(5) Tinker, A. C.; Wallace, A. V. Selective inhibitors of inducible nitric oxide synthase: potential agents for the treatment of inflammatory diseases? *Curr. Top. Med. Chem.* **2006**, *6*, 77−92.
(6) Pacher, P.; Bechman, J. S.; Liaudet, L. Nitric oxide and peroxynitrite in health and disease. *Physiol. Rev.* **2007**, *87*, 315−324.
(7) Liaudet, L.; Rosenblatt-Velin, L.; Pacher, P. Role of the peroxynitrite in the cardiovascular dysfunction of septic shock. *Curr. Vasc. Pharmacol.* **2013**, *11*, 196−207.
(8) Roos, A. B.; Mori, M.; Gronneberg, R.; Osterlund, C.; Claesson, H. E.; Wahlstrom, J.; Grunewald, J.; Eklund, A.; S Erjefalt, J.; O Lundberg, J.; Nord, M. Elevated exhaled Nitric Oxide in allergen-provoked asthma is associated with airway epithelial iNOS. *PLoS One* **2014**, *9*, 1−8.
(9) Oliveira-Paula, G. H.; Lacchini, R.; Tanus-Santos, J. E. Inducible nitric oxide synthase as a possible target in hypertension. *Curr. Drug. Targets* **2014**, *15*, 164−174.
(10) Cross, R. K.; Wilson, K. T. Nitric oxide in inflammatory bowel disease. *Inflamm. Bowel Dis.* **2003**, *9*, 179−189.
(11) Belgorosky, D.; Langle, Y.; Prack McCormick, B.; Colombo, L.; Sandes, E.; Eiján, A. M. Inhibition of nitric oxide is a good therapeutic target for bladder tumors that express iNOS. *Nitric Oxide* **2014**, *36*, 11−18.
(12) Pandolfi, A.; De Filippis, E. A. Chronic hyperglicemia and nitric oxide bioavailability play a pivotal role in pro-atherogenic vascular modifications. *Genes Nutr.* **2007**, *2*, 195−208.
(13) Joubert, J.; Malan, S. F. Novel nitric oxide synthase inhibitors: a patent review. *Expert Opin. Ther. Pat.* **2011**, *21*, 537−560.
(14) Tafi, A.; Angeli, L.; Venturini, G.; Travagli, M.; Corelli, F.; Botta, M. Computational studies of competitive inhibitors of nitric oxide synthase (NOS) enzymes: towards the development of powerful and isoform-selective inhibitors. *Curr. Med. Chem.* **2006**, *13*, 1929−1946.
(15) Maccallini, C.; Fantacuzzi, M.; Amoroso, R. Amidine-based bioactive compounds for the regulation of arginine metabolism. *Mini-Rev. Med. Chem.* **2013**, *13*, 1305−1310.
(16) Maccallini, C.; Patruno, A.; Besker, N.; Ali, J. I.; Ammazzalorso, A.; De Filippis, B.; Franceschelli, S.; Giampietro, L.; Pesce, M.; Reale, M.; Tricca, M. L.; Re, N.; Felaco, M.; Amoroso, R. Synthesis, biological evaluation, and docking studies of N-substituted acetamidines as selective inhibitors of inducible nitric oxide synthase. *J. Med. Chem.* **2009**, *52*, 1481−1485.
(17) Maccallini, C.; Patruno, A.; Lannutti, F.; Ammazzalorso, A.; De Filippis, B.; Franceschelli, S.; Fantacuzzi, M.; Giampietro, L.; Masella, S.; Felaco, M.; Re, N.; Amoroso, R. N-Substituted acetamidines and 2-methylimidazole derivatives as selective inhibitors of neuronal nitric oxide synthase. *Bioorg. Med. Chem. Lett.* **2010**, *20*, 6495−6499.
(18) Fantacuzzi, M.; Maccallini, C.; Lannutti, F.; Patruno, A.; Masella, S.; Pesce, M.; Speranza, L.; Ammazzalorso, A.; De Filippis, B.; Giampietro, L.; Re, N.; Amoroso, R. Selective inhibition of iNOS by benzyl- and dibenzyl derivatives of N-(3-aminobenzyl)acetamidine. *ChemMedChem* **2011**, *6*, 1203−1206.
(19) Maccallini, C.; Patruno, A.; Ammazzalorso, A.; De Filippis, B.; Fantacuzzi, M.; Franceschelli, S.; Giampietro, L.; Masella, S.; Tricca, M. L.; Amoroso, R. Selective inhibition of inducible nitric oxide synthase by derivatives of acetamidine. *Med. Chem.* **2012**, *8*, 991−995.
(20) Zhu, Y.; Nikolic, D.; Van Breemen, R. B.; Silverman, R. B. Mechanism of inactivation of inducible nitric oxide synthase by amidines. Irreversible enzyme inactivation without inactivator modification. *J. Am. Chem. Soc.* **2005**, *127*, 858−868.
(21) Haitao, J.; Huiying, L.; Flinspach, M.; Poulos, T. L.; Silverman, R. B. Computer modeling of selective regions in the active site of nitric oxide synthases: implication for the design of isoform-selective inhibitors. *J. Med. Chem.* **2003**, *46*, 5700−5711.
(22) Montagnani, M.; Potenza, M. A.; Rinaldi, R.; Mansi, G.; Nacci, C.; Serio, M.; Vulpis, V.; Pirrelli, A.; Mitolo-chieppa, D. Functional characterization of endothelin receptors in hypertensive resistance vessels. *J. Hypertens.* **1999**, *17*, 45−52.
(23) Mitolo-Chieppa, D.; Serio, M.; Potenza, M. A.; Montagnani, M.; Mansi, G.; Pece, S.; Jirillo, E.; Stoclet, J. C. Hyporeactivity of mesenteric vascular bed in endotoxin-treated rats. *Eur. J. Pharmacol.* **1996**, *309*, 175−182.
(24) Milletti, F.; Storchi, L.; Sforna, G.; Cruciani, G. New and original pka prediction method using of GRID molecular interaction fields. *J. Chem. Inf. Model.* **2007**, *47*, 2172−2181.
(25) Milletti, F.; Storchi, L.; Goracci, L.; Bendels, S.; Wagner, B.; Kansy, M.; Cruciani, G. Extending pKa prediction accuracy: high-throughput pKa measurements to understand pKa modulation of new chemical series. *Eur. J. Med. Chem.* **2010**, *45*, 4270−4279.
(26) Computational methods and software references are detailed in the Supporting Information.

DOI: 10.1021/acsmedchemlett.5b00149
ACS Med. Chem. Lett. 2015, 6, 635−640